A Snake Toxin Inhibitor of Inward Rectifier Potassium Channel ROMK1†

John P. Imredy,‡ Chinfei Chen,§ and Roderick MacKinnon*,‡

Howard Hughes Medical Institute and Laboratory of Molecular Neurobiology and Biophysics, Rockefeller University, New York, New York 10021, and Department of Neurobiology, Harvard Medical School, 220 Longwood Avenue, Boston, Massachusetts 02115

Received April 23, 1998; Revised Manuscript Received July 20, 1998

ABSTRACT: Mamba snake dendrotoxins have been used extensively in biochemical and physiological studies of K^+ channels of the brain. Their known targets of inhibition have been limited to the family of voltage-gated K^+ channels. We report the isolation of a dendrotoxin inhibitor of ROMK1, a channel belonging to the inward rectifier family of K^+ channels. The inhibitory activity, fractionated to purity with FPLC and HPLC, is identical to a previously identified δ-dendrotoxin. To verify that δ-dendrotoxin blocks ROMK1 channels, a cDNA encoding the toxin was synthesized and recombinant toxin expressed in *Escherichia coli*. Electrophysiological recordings reveal that recombinant δ-dendrotoxin has a half-maximal inhibition constant (K_d) of 150 nM when applied to ROMK1 channels expressed in *Xenopus laevis* oocytes. That the δ-dendrotoxin binding site exists on separate K^+ channel classes is shown by its high affinity for two of the voltage-gated family of channels, Kv1.1 (K_d < 0.1 nM) and Kv1.6 (K_d = 23 nM). Single amino acid substitutions in ROMK1 indicate that δ-dendrotoxin binds to the pore region of ROMK1 even though it does not completely block conduction through the pore. These results suggest that dendrotoxins inhibit K^+ channels by recognizing the structurally conserved pore region of these channels.

Inward rectifiers constitute a class of K^+ channels that play an important role in modulating repetitive firing, permitting long depolarizing responses, and maintaining the resting potential near E_K (the reversal potential for K^+) in cardiac, smooth muscle, neuronal, and endocrine cells (*1*, *2*). As their name implies, most inward rectifiers conduct K^+ asymmetrically: K^+ influx into the cell at negative membrane voltages is kinetically favored over K^+ efflux at positive voltages.

cDNAs encoding inward rectifier K^+ channels have been isolated from renal cells [ROMK1, (*3*)],[1] a macrophage cell line [IRK1, (*4*)], cardiac cells [GIRK1, (*5*); hIRK, (*6*); CIR, (*7*)], and neuronal cells [HRK1, (*8*); MB-IRK2, (*9*)]. Their deduced amino acid sequences suggest that they share structural properties which set them apart from the voltage-gated K^+ channels. In contrast to the six membrane-spanning hydrophobic amino acid stretches of the voltage-gated family of K^+ channels (S1−S6) (*10*), inward rectifier K^+ channels have only two hydrophobic stretches, the inner and outer transmembrane helices (*11*). Their inward rectification is a result of blockade by impermeant intracellular cations (*12*, *13*).

Specific high-affinity toxins have been used as tools to understand the structure and function of the voltage-gated family of channels. Scorpion toxins have been used to identify the pore region (*14*, *15*), determine the subunit stoichiometry (*16*), and elucidate the topology of the extracellular face of the channel pore (*17*−*25*). The structural interactions between K^+ channels and dendrotoxins are less well understood though they have allowed mapping of the neuroanatomical distribution of voltage-gated K^+channels (*26*) and isolation of native K^+channel complexes from the brain (*27*, *28*). α-Dendrotoxin has been shown to interact with residues in the pore region of voltage-gated K^+ channel Kv1.1 (*29*−*31*). No dendrotoxin has been shown to interact with K^+ channels outside the voltage-gated family (*32*). The recent determination of a K^+ channel structure (*11*), together with a refined understanding of how dendrotoxins may interact with such channels, promises to reveal new information about the molecular interaction of dendrotoxins with K^+ channels.

EXPERIMENTAL PROCEDURES

Purification of Crude Venom and Peptide Analysis. Lyophilized venom from the snake *Dendroaspis angusticeps* (Latoxan, France) was suspended in distilled water up to a concentration of 25 mg/mL. The following steps were carried out at room temperature. The solution was vortexed and centrifuged at 27000*g* for 15 min, and the supernatant was filtered through a 0.2 μm filter. This venom mixture was then injected onto a MonoS (HR 10/10) FPLC column (Pharmacia) which had previously been equilibrated with column buffer: 20 mM sodium phosphate, pH 8.0. The injected venom was eluted with a linear gradient of NaCl

† This research was funded by NIH Grant GM43949. C.C. was supported by a Howard Hughes Physician Postdoctoral Fellowship. R.M. is an Investigator in the Howard Hughes Medical Institute.

* Correspondence should be addressed to this author at Box 47, 1230 York Ave., New York, NY 10021. Telephone (212) 327-7288. FAX: (212) 327-7289. E-mail: mackinn@rockvax.rockefeller.edu.

‡ Rockefeller University.

§ Harvard Medical School.

[1] Abbreviations: ROMK1, renal outer medulla inward rectifier potassium channel; FPLC, fast protein liquid chromatography; HPLC, high-performance liquid chromatography; SDS−PAGE, sodium dodecyl sulfate−polyacrylamide gel electrophoresis; BSA, bovine serum albumin; HEPES, 4-(2-hydroxyethyl)-1-piperazineethanesulfonic acid; TRIS, tris(hydroxymethyl)aminomethane.

10.1021/bi980929k CCC: $15.00
Published on Web 09/26/1998

added to the column buffer, reaching 1 M over a 40−60 min period at a flow rate of 2 mL/min. The UV absorbance at 280 nm of the eluate was continuously monitored. Fractions of high absorbance were diluted 10−100-fold in electrophysiological recording solution (see below) and assayed for inhibitory activity on ROMK1 current expressed in oocytes (Figure 1). Only one fraction, which eluted at ∼0.64 M NaCl, blocked the inward rectifier current by more than 5%. This fraction was injected onto a C18 (Vydac 218TP54, 5 μm, 80 Å) or C8 (Vydac 208TP54, 5 μm, 300 Å) reverse-phase HPLC column which had been equilibrated with distilled water. The inhibitor was eluted with a linear gradient of acetonitrile (0−60%/60 min) at a flow rate of 0.5 mL/min; 0.1% trifluoroacetic acid was added to all HPLC solutions as the reverse-phase counterion. δ-Dendrotoxin eluted as a single large peak at ∼30% acetonitrile. This peak was collected and lyophilized, resuspended in distilled water, and relyophilized to reduce residual TFA. The lyophilized inhibitor was stored at −80 °C.

The amino acid content of the inhibitor was quantified by amino acid analysis after automated hydrolysis and derivatization with phenylisothiocyanate (PTC). The PTC-amino acids were separated on a HPLC system, using a C18 reverse-phase column and NaHOAc/acetonitrile gradients. Chromatograms of samples and calibrated standards were evaluated to determine the amount of samples hydrolyzed, and the extinction coefficient was calculated as 17 883 cm^{-1} M^{-1}. For protein sequencing, the purifed inhibitor from venom was treated with 4-vinylpyridine and sequenced using automated Edman degradation. Amino acid analysis, peptide sequencing, and mass spectrometry were carried out at the Harvard HHMI Biopolymer Facility.

Recombinant Toxin Synthesis. A synthetic gene encoding δ-dendrotoxin was designed such that a factor Xa cleavage site peptide sequence (Iso-Glu-Gly-Arg-) immediately preceded the N-terminal alanine of the toxin (Figure 2). The factor Xa cleavage site was preceded with a *Sal*I restriction site at the gene 5′ end. A *Hin*dIII restriction site followed the stop codon of the toxin at the gene 3′ end. Four oligonucleotides, each approximately 70 bases long and alternating between sense and antisense strands, were synthesized such that there was a 15 base pair overlap between consecutive strands. The full-length gene was synthesized in a PCR reaction containing 10 pmol each of the four oligonucleotides and 300 pmol each of sense and antisense primer at the 5′ and 3′ ends of the gene sequence. The sense strand, of which restriction sites *Sal*I and *Hin*dIII are italicized, was as follows: 5′-GCGGGATCCTCGAGCTCG*GTCGAC*ATCGAGGGACGTGCTGCTAAGTACTGTAAGCTCCCTGTCAGGTACGGACCTTGTAAGAAGAAGATCCCTTCTTTCTACTACAAGTGGAAGGCTAAGCAATGTCTTCCTTTTGATTACAGTGGATGCGGCGGCAACGCGAATCGATTTAAGACCATCGAAGAGTGTCGAAGGACCTGTGTCGGCTGAGAAC*AAGCTT*GAATTCC-3′. The gene was subcloned into vector pCSP105 (*33*) using *Sal*I and *Hin*dIII restriction sites and the insert confirmed by sequencing (*34*). This vector expresses δ-dendrotoxin as a C-terminal fusion to the bacteriophage T7 capsid protein (gene 9 product)(*35*).

The fusion protein was expressed in *E. coli* strain BL21-DE3 and harvested according to Park et al. (*33*). All subsequent purification steps were carried out at 4 °C. The fusion protein was precipitated with ammonium sulfate, resuspended in 50 mM NaCl, 5 mM 2-mercaptoethanol, 50 mM TRIS, pH 8.0 (HCl), and purified using anion exchange chromatography on a Whatman DE52 cellulose packed column using a NaCl gradient [50−500 mM NaCl, 5 mM 2-mercaptoethanol, 50 mM TRIS, pH 8.0 (HCl)]. Fractions containing the fusion protein, as identified by Coomassie Blue staining of SDS−PAGE gels, were pooled and dialyzed against 10 mM TRIS, 0.5 mM 2-mercaptoethanol, pH 7.5 (HCl). Before enzymatic cleavage, 100 mM NaCl and 1 mM $CaCl_2$ were added to the dialysate. Cleaving the δ-dendrotoxin from the fusion protein at the factor Xa recognition site required a 24 h, 22 °C, incubation with factor Xa [1 μg of factor Xa per 100 μg of fusion protein (based on a calculated 280 nm absorbance extinction coefficient of 32 mM^{-1} cm^{-1} for the fusion protein)]. Cleavage by trypsin (1 μg/100 μg of fusion protein) was equally successful, yielding an identical peptide according to mass spectrometry and inhibition of expressed ROMK1 current. Serial digestions with trypsin revealed an optimal incubation period of 1 h 15 min at 22 °C. Longer incubations resulted in progressively smaller yields. Further purification of recombinant δ-dendrotoxin from the cleavage mixture was achieved using the same combination of FPLC cation exchange (at 4 °C) and reverse-phase HPLC chromatography as in the procedure described for native toxin (see above).

Scorpion toxin LQ2 was prepared according to Lu and MacKinnon (*25*) and was a gift of Dr. Lu.

Expression of Ion Channels. Oocytes from *Xenopus laevis* were prepared and injected with cRNA transcribed from the following linearized DNA plasmids according to Lu and MacKinnon (*25*). The ROMK1 cDNA, in p-SPORT1 plasmid, was kindly provided by Drs. Ho and Hebert (*3*). Channel genes encoding IRK1 (*4*), Shaker (*36*), Kv1.1 (*37*), and Kv1.6 (*38*) cDNAs were subcloned into and transcribed from pcDNA/Amp (Invitrogen), pBluescript (Stratagene), pGEM-3z, and pGEM-9fz(−) vectors (Promega), respectively. RNA was synthesized using either T7 or T3 RNA polymerase transcription kits (Promega). cDNAs encoding mutant ROMK1 channels were previously prepared (*25*).

Electrophysiology. (Whole cell) Oocytes were placed in a 130 μL bath into which ND96 solution was continuously perfused [ND96: 96 mM NaCl, 2 mM KCl, 1.8 mM $CaCl_2$, 1 mM $MgCl_2$, 5 mM HEPES, pH 7.6 (NaOH)]. Glass capillary electrodes (World Precision Instruments, TW100F-6) were pulled to resistances ranging from 0.3 to 0.8 MΩ when filled with 3 M KCl. After impaling the oocyte, the resting voltage of the oocyte was noted (< −75 mV). After stabilization of the resting potential, the perfusate was changed to the recording solution. For measurement of inward rectifier current (ROMK1 and IRK1), the recording solution consisted of 100 mM KCl, 0.3 mM $CaCl_2$, 1 mM $MgCl_2$, 10 mM HEPES, pH 7.4 (KOH). Once equilibrated with the high K^+ solution, the resting potential increased to near 0 mV. Hyperpolarizing pulses from a holding potential of 0 mV to either −80 or −60 mV, lasting 200 ms, were applied by the two-electrode voltage-clamp amplifier (Warner Instruments, OC-725B) under control of a personal computer. The K^+ current signal was low-pass-filtered at 0.6 kHz cutoff, sampled at intervals of 0.5−1 ms, and digitized and stored on computer disk. Voltage-gated K^+ channel currents

(Shaker, Kv1.1, Kv1.6) were recorded from oocytes perfused continuously with ND96 solution (see above). Voltage-dependent currents were elicited by stepping from a holding potential of −90 to 0 mV for a duration of 200 ms. For all channels, the average current value during the last 15 ms of the voltage pulse was used to determine fractional inhibition. K_d was calculated assuming 1:1 binding. All channel recordings were obtained at room temperature.

In whole cell experiments involving purified native or recombinant toxin, 0.1 mg/mL BSA was added to all solutions to minimize nonspecific toxin binding. Prior to electrophysiological recording, a small amount of lyophilized toxin (−80 °C) was reconstituted at a high concentration into 100 mM K-HEPES, pH 7.4, and the concentration determined using UV absorbance at 280 nm. The solubilized toxin was stored on ice for the remainder of the experiment. Concentrated toxin was diluted to the desired concentration into a reservoir of recording solution immediately before perfusion into the oocyte bath chamber. Only oocytes expressing currents between 1 and 5 μA were used to obtain K_d values.

(Single channel) Oocytes were devitellinated in ND96 solution using fine forceps. Single-channel patch electrodes (Warner Instruments, GT15) were pulled and fire-polished to resistances of 1−2 MΩ and coated with melted bee's wax. Oocytes were continuously perfused with high K^+ recording solution, and it was assumed that the intracellular potential was 0 mV (see above) for on-cell single-channel recording. Patch pipets were filled with the same recording solution containing 0.1 mg/mL BSA and toxin, if applicable. In single-channel patches with Ba^{2+} present, 0.01 mM $BaCl_2$ was added to the recording solution in the patch pipet. In experiments with Ba^{2+} and toxin, the pipet tip was first dipped into recording solution to which 0.01 mM $BaCl_2$ had been added (without BSA), and then back-filled with recording solution containing 0.01 mM $BaCl_2$ and 1.0 μM toxin. This ensured that the blocking action of Ba^{2+} could be identified in isolation before onset of toxin-induced closures. Single ROMK1channel currents were obtained using an Axopatch 200A amplifier (Axon Instruments) in the capacitative feedback mode, holding the potential of the patch continuously at −80 mV (inside-out configuration). The current signal was low-pass-filtered at 1 kHz and sampled at 0.2 ms intervals. Closed and open time durations of the channel were calculated using half-unitary amplitude crossings of the raw current trace.

RESULTS

Crude venom from the South African green mamba snake, *Dendroaspsis angusticeps*, was applied to *Xenopus laevis* oocytes expressing ROMK1 currents (Figure 1C). This initial screening of the venom was performed with ROMK1 channels in which asparagine 171 in the inner helix (*11*) was replaced by aspartate. This mutant carries very little outward current at depolarized potentials and thus rectifies more strongly than wild-type ROMK1 (*12*). Use of this mutant allowed a clearer distinction between endogenous outward currents present in oocytes at positive potentials and the ROMK1 current. It has been shown that this mutation does not affect the extracellular pore region of the channel (*25*). Figure 1C demonstrates the inhibitory activity of 0.4 mg/mL whole venom when perfused onto N171D ROMK1 K^+ current expressing oocytes recorded while stepping the voltage of the oocyte membrane to −80 mV from a holding potential of 0 mV. A depolarizing pulse to 80 mV immediately followed the pulse to −80 mV. The smaller outward currents during the depolarizing pulse illustrate the rectifying property of this channel. The large current transients at the beginning of the voltage steps are not ROMK1 currents but are due to the capacitative currents needed to charge the large surface area of the oocyte membrane. Standard leak subtraction protocols used to cancel linear capacitative currents were not applicable since ROMK1 channels are continuously open and lack voltage-dependent gating.

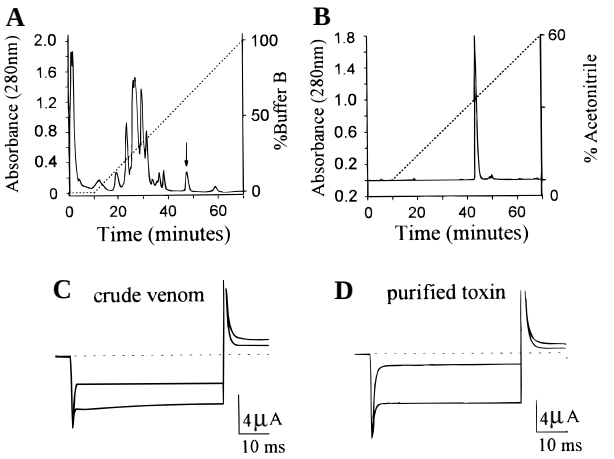

FIGURE 1: Purification of ROMK1 inward rectifier inhibitory activity. (A) 280 nm wavelength light absorbance of eluate during cation-exchange chromatography of crude venom from *dendroapsis angusticeps*. 25 mg of lyophilized venom was dissolved in 1 mL of distilled water and injected onto a Mono S column equilibrated with buffer A. The column was exposed to a linear gradient from 0 to 100% buffer B over 60 min (dashed line). Buffer A: 20 mM NaH_2PO_4, pH 8.0. Buffer B: 1 M NaCl, 20 mM NaH_2PO_4, pH 8.0. The arrow shows the peak which contained inhibitory activity to ROMK1 current. (B) Reverse-phase HPLC of the active fraction from the MonoS column. One major peak was eluted using a gradient of 0−60% acetonitrile over 60 min (dashed line). Buffer A: 0.1% trifluoroacetic acid (TFA) in distilled water. Buffer B: 0.1% TFA in acetonitrile. (C) Effect of crude venom on ROMK1 N171D currents. K^+ currents elicited with a hyperpolarizing step from 0 to −80 mV, followed by a depolarizing step to +80 mV. Bath perfusion of 0.4 mg/mL crude venom inhibited both the inward and outward components of the ROMK1 current. (D) The major peak from HPLC purification (B) inhibits ROMK1 N171D current. A 0.64 μg/mL aliquot of the FPLC/HPLC purified fraction inhibits the inward rectifying current at both −80 and +80 mV. (C and D) Dashed lines indicate zero current level.

A two-step purification of the inhibitory activity was developed using the assay system described above. The first step is a fractionation of crude venom on a cation exchange column (Figure 1A). Fractions of 2−4 mL of eluate were collected sequentially and tested individually at a dilution of 1:100 and 1:10 against the ROMK1 current. Only a single isolated fraction, separated from most other fractions by a higher retention time, blocked ROMK1 K^+ current by more than 5% (Figure 1A, arrow). Figure 1B shows that the peak isolated from the cation exchange column is essentially pure as it also runs as a single peak on a reverse-phase column. This major peak contained the ROMK1 inhibitor (Figure 1D).

Mass spectrometry of the purified fraction revealed a 6590 Da molecule. The results of amino acid analysis in Table 1

Table 1: Amino Acid Analysis[a] of ROMK1 Inhibitor

amino acid	residues/molecule observed	residues/molecule δ-dendrotoxin
aspartic acid, asparagine	3.0	3
glutamic acid, glutamine	3.0	3
serine	2.0	2
glycine	5.0	5
histidine	0.2	0
arginine	4.3	4
threonine	2.0	2
alanine	4.3	4
proline	4.4	4
tyrosine	4.8	5
valine	1.9	2
methionine	0.1	0
isoleucine	1.7	2
leucine	2.1	2
phenylalanine	3.1	3
lysine	9.0	9

[a] See Experimental Procedures. Cysteine and tryptophan residues were not detected by this technique.

FIGURE 2: ROMK1 inhibitor corresponds to δ-dendrotoxin. Amino acid sequence of δ-dendrotoxin. Shown are the cysteine bonds and the secondary structural characteristics determined from the solved crystallographic and NMR structures of dendrotoxins (*45*, *46*).

are shown along with the number of each amino acid present in δ-dendrotoxin (*39*). Peptide sequencing of the first 53 amino acids from the N-terminus yielded a perfect match with the first 53 amino acids (Figure 2) of a previously identified δ-dendrotoxin which has a predicted mass of 6573 Da. There are a total of 13 basic residues (Arg and Lys) and 3 acidic residues (Glu and Asp). This toxin was first identified and sequenced in 1980 (*39*) and shown to alter rubidium fluxes in rat brain synaptosomes (*40*). It inhibits voltage-dependent, outward K^+ currents in rat neurons (*41*), and recently, a specific interaction with expressed mouse Kv1.1 channels has been described (*42*). There is no previous report of this peptide's effect on K^+ channels of the inward rectifier family. The effect of δ-dendrotoxin on ROMK1 appeared to be specific since α-dendrotoxin, a related peptide from the same venom, blocked the ROMK1 current by less than 10% at 1 μM (data not shown).

Synthesis of Recombinant δ-Dendrotoxin. To verify that δ-dendrotoxin blocks the inward rectifier ROMK1, we synthesized recombinant toxin. A synthetic gene based on the amino acid sequence of δ-dendrotoxin was subcloned into an *E. coli* expression vector, pCSP105 (*33*), as a C-terminal fusion to the capsid protein of bacteriophage T7 (gene 9 product) (*35*). The toxin was cleaved from the fusion protein at an engineered protease recognition site by either factor Xa or trypsin. Both proteases cleaved at the same site as determined by mass spectrometry, and the affinity of both toxin cleavage products for expressed ROMK1 channels was the same (data not shown). Recombinant toxin was separated from the proteolytic mixture by FPLC cation exchange chromatography. Finally, desalting and further

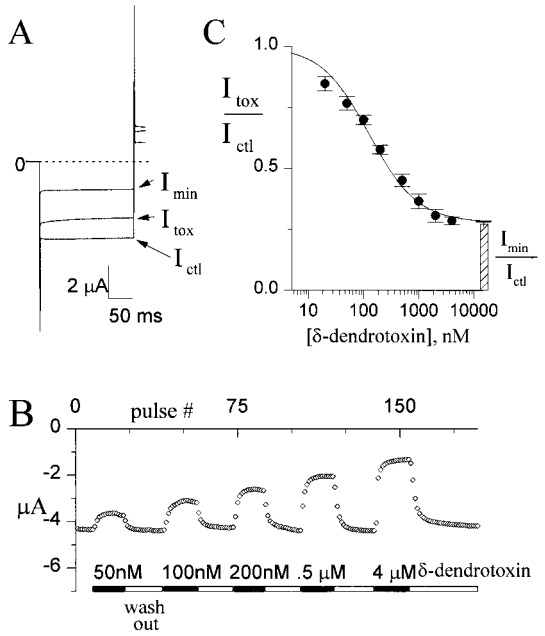

FIGURE 3: Concentration dependence of δ-dendrotoxin inhibition of ROMK1. (A) ROMK1 currents in response to a voltage pulse to −60 mV of 200 ms duration followed by a 30 ms pulse to +60 mV. Holding potential is 0 mV. Shown are three current traces taken from the same oocyte. I_{ctl}, wild-type ROMK1 current in the absence of toxin; I_{tox} and I_{min}, wild-type ROMK1 current equilibrated with 100 nM and 10 μM δ-dendrotoxin, respectively. (B) Progression of a blocking experiment. Same oocyte as in (A). Each diamond (◊) plots the average ROMK1 K^+ current during the final 15 ms of the voltage pulse to −60 mV in the continuously repeated protocol described in (A). The interval between successive pulse protocols is 7 s. Same oocyte as in (A). Perfusions of increasingly higher concentrations of toxin (black horizontal bars, with indicated concentrations) were each followed by wash with toxin-free solution (white bars). (C) Filled circles (●) plot the average remaining inward current fraction, I_{tox}/I_{ctl}, after equilibration of δ-dendrotoxin block at the following applied concentrations: 20, 50, 100, 500, 1000, 2000, and 4000 nM δ-dendrotoxin. Each point is the mean ± SEM, $n = 18$ oocytes. The smooth curve is a least-squares fit of $\beta + (1 - \beta)[1 + ([\delta\text{-dendrotoxin}]/K_d)]^{-1}$, where $K_d = 150$ and $\beta = 0.28$. The bar shows the average toxin-insensitive fraction of ROMK1 currents, I_{min}/I_{ctl}, ± SEM, from the same 18 cells.

purification of the toxin were achieved by HPLC reverse-phase chromatography using the procedures described for native toxin. This expression method yielded 0.5−1 mg of recombinant δ-dendrotoxin per liter of culture volume. The final recombinant peptide had a biochemical profile similar to native toxin on mass spectrometry (6577 Da). Co-injection of equimolar amounts of native and recombinant toxin on reverse-phase HPLC eluted as a single peak (not shown).

Functional Activity of Recombinant δ-Dendrotoxin. Subsequent functional studies of δ-dendrotoxin were carried out using the recombinant toxin and wild-type ROMK1 channel. Figure 3A illustrates the reduction of inward wild-type ROMK1 K^+current (I_{ctl}) after application and equilibration of the channels with 100 nM δ-dendrotoxin (I_{tox}) and then 10 μM δ-dendrotoxin (I_{min}). Figure 3B shows the progression of such an experiment. Plotted is the average inward current during the last 15 ms of steps to −60 mV from a holding potential of 0 mV, repeated every 7 s. The oocyte was continuously perfused with solutions containing increasingly higher concentrations of δ-dendrotoxin followed by a wash. Removal of the toxin after equilibration of toxin

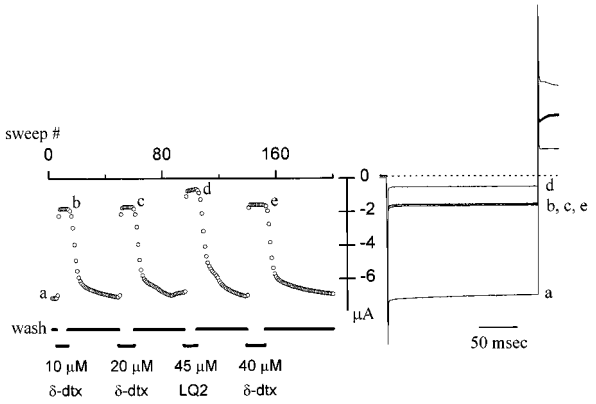

FIGURE 4: Comparison of scorpion toxin LQ2 and δ-dendrotoxin at near saturating concentrations. Illustrated is an experiment comparing the degree of block of ROMK1 current by near-saturating amounts of both δ-dendrotoxin (K_d = 150 nM) and LQ2 toxin (from scorpion *Leiurus quinquestriatus*, K_d = 0.4 μM.) The protocol was identical to that of Figure 3. The right panel illustrates the ROMK1 currents elicited by voltage steps at the different conditions during the experiment (a−e). Open circles (○) in the left panel show the average currents during the last 15 ms of the steps to −60 mV. The small letters refer to the following conditions: (a) control without toxin; (b and c) 10 and 20 μM δ-dendrotoxin, respectively; (d) 45 μM scorpion LQ2 toxin; and (e) 40 μM δ-dendrotoxin. Each application of toxin (lower horizontal line) was followed by removal (upper horizontal line, left panel).

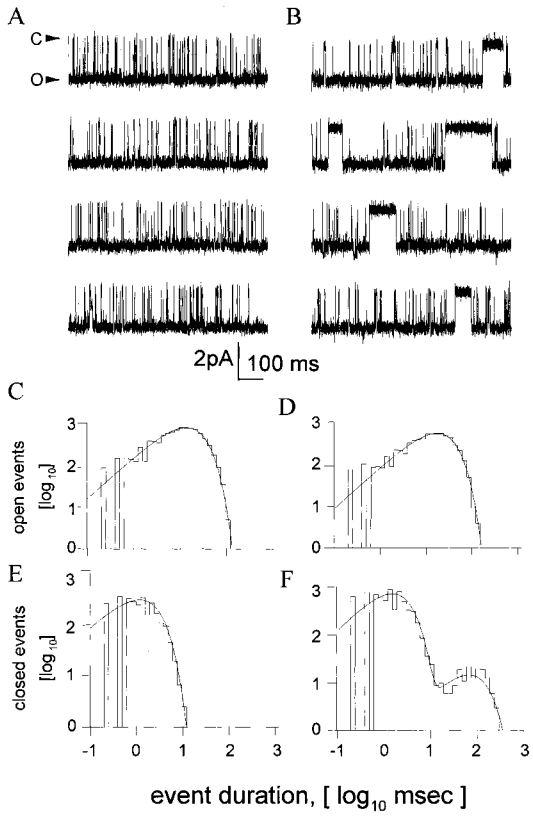

FIGURE 5: Characteristics of δ-dendrotoxin inhibition of single ROMK1 channels. (A) Continuous 3.3 s on-cell recording of a single ROMK1channel held at −80 mV. C and O indicate that channel opening is in the downward direction (inward current) at −80 mV. (B) Same as (A) but now with 50 nM δ-dendrotoxin added to the pipet filling solution (extracellular face of channel). Toxin blocking events are long sojourns near the closed channel current. Five blocking and unblocking events were observed during the displayed 3.3 s period. Single-channel currents in (A) and (B) were sampled at 5 kHz and low-pass-filtered at 1 kHz. (C) Histogram of open time durations during a 2.3 min continuous recording of the channel in (A). Open time durations were binned into logarithmically increasing bin widths (25 bins/decade). The smooth curve shows the fit of a single decaying exponential, $A_1 \exp(-t/\tau_1)$, to the distribution (A_1 = 927, τ_1 = 13.2 ms). (D) Same as (C) but for toxin-exposed channel in (B) (A_1 = 673, τ_1 = 15.7 ms). (E) Histogram of closed time durations of the channel shown in (A) over the same 2.3 min period as used in (C). Single-exponential fit (A_1 = 1300, τ_1 = 1.0 ms). (F) Same as (E) but for toxin-exposed channel in (B). A sum of two decaying exponentials was used to fit this distribution, $A_1 \exp(-t/\tau_1) + A_2 \exp(-t/\tau_2)$ (A_1 = 638, τ_1 = 1.58 ms; A_2 = 18, τ_2 = 79.4 ms). The time constant of the more slowly decaying exponential, ∼80 ms, describes the average binding duration of the toxin to the channel. Bath solution, K^+ recording solution (see Experimental Procedures) without bovine serum albumin. Pipet solution, K^+ recording solution with or without toxin.

binding at each applied concentration fully restored the K^+ current to its original base line level (wash out). After a series of such applications, concentrated toxin was added to the recording chamber until the inward current remained unchanged with further addition of toxin (not shown). The remaining toxin-insensitive current was considered the leak current, I_{min}. The concentration dependence of fractional inhibition of ROMK1 current by recombinant δ-dendrotoxin is shown in Figure 3C. The data were fit with a Langmuir isotherm function (see Figure 3 legend) assuming 1:1 binding between the ROMK1 channel and δ-dendrotoxin with an equilibrium dissociation constant (K_d) of 150 nM.

The leak current, I_{min}, was always a substantial fraction of total current ($0.18I_{ctl} \leq I_{min} \leq 0.36I_{ctl}$, average $I_{min} = 0.27I_{ctl}$, Figure 3B, bar) and suggested that δ-dendrotoxin, when bound to the channel, is not able to completely inhibit the ionic flux through the channel.

The possibility exists that the incomplete block of inward current arises due to a toxin-insensitive fraction of expressed channels. Perhaps the same endogenous oocyte inward rectifier, XIR, shown to be induced by expression of G-protein-regulated inward rectifier (GIRK) isotypes in oocytes (*43*), may have been induced during our expression of ROMK1, resulting in an inhomogeneous channel population. To investigate the identity of the toxin-resistant current fraction, we applied LQ2 toxin. This 37 amino acid toxin, which belongs to the charybdotoxin and agitoxin family of scorpion inhibitors, has recently been shown to block ROMK1 currents expressed in *Xenopus* oocytes (*25*). Figure 4 compares near-saturating concentrations of δ-dendrotoxin and LQ2 (K_d = 0.4 μM). The first two applications (Figure 4, b,c) of δ-dendrotoxin reveal the inability of δ-dendrotoxin to block a substantial (25%) fraction of the expressed ROMK1 current (Figure 4, a). In contrast, LQ2 blocked more than 90% of the control current (Figure 4, d). That both LQ2 and δ-dendrotoxin compete for the same binding sites was shown by first applying LQ2 to saturation and then, without an intervening wash, adding δ-dendrotoxin. As would be expected for competitive inhibitors, the maximally blocked current increased to a value intermediate between 10% and 25% (not shown). These results argue that wild-type δ-dendrotoxin when bound to ROMK1 may not completely prevent current flux through the channel.

To further analyze the dendrotoxin−ROMK1 interaction, single channels were examined (Figure 5). Oocyte-attached membrane patches were recorded for ROMK1 channel activity using the same solution as in the bath in Figure 3,

but now in the patch pipet. Figure 5A shows K^+ current flowing through a single ROMK1 channel held continuously at −80 mV. The ROMK1 channel remains open except for intermittent brief closures on the order of a fraction of a millisecond (Figure 5A). Histograms of open and closed times are illustrated in Figure 5C and Figure 5E, respectively. Single decaying exponentials were fit to each of the histograms.

After addition of δ-dendrotoxin to the patch pipet solution, the open channel activity is interrupted by discrete long-lived closures (Figure 5B). The closures introduce a second component into the distribution of channel closed times (Figure 5F, time constant ≈ 80 ms). The average open time duration remains virtually identical in the presence of toxin (Figure 5C vs 5D). The discrete blocking events of ROMK1 were well resolved, and addition of higher toxin concentrations to the pipet solution resulted in shorter intervals between successive blocks (data not shown). These effects are consistent with a bimolecular interaction of channel and toxin.

To clarify the issue of whether δ-dendrotoxin is an incomplete ROMK1 K^+ channel blocker as suggested by the two-electrode voltage-clamp studies, we compared blocks of the K^+ channel by Ba^{2+} to blocks by δ-dendrotoxin. Ba^{2+} blocks ROMK1, introducing long closures (Figure 6A,B). When toxin as well as Ba^{2+} was present at the patch, an additional type of incomplete closure was observed (Figure 6C,D). Comparison of amplitude histograms of these two types of closures (complete blocks induced by Ba^{2+} and partial blocks induced by toxin) indicates that the dendrotoxin-blocked channel conducts K^+ at roughly one-tenth the rate of the open channel (Figure 6D). Interestingly, Ba^{2+} and toxin occupancy of the channel were not mutually exclusive as toxin-induced subconductance states could be interrupted by transitions to zero conductance states associated with Ba^{2+} blockade (Figure 6E). Similarly, the toxin was able to bind the channel while Ba^{2+} occupied the selectivity filter as shown by the direct transitions from the zero-conductance to the toxin-associated subconductance state. The apparent large discrepancy between the single-channel unblocked fraction of ∼10% and the toxin-resistant whole cell fraction (∼25%, Figure 3) may be explained by the existence of an unidentified leak current even in the presence of saturating LQ2 concentrations (Figure 4) (*25*) which, when subtracted from the whole cell fraction, leaves only 15% of dendrotoxin-insensitive whole cell ROMK1 current.

Specificity of δ-Dendrotoxin. Figure 7 (right panel) shows the K_d of recombinant δ-dendrotoxin for several different K^+ channels. These channels were expressed in X*enopus* oocytes, and their affinities for δ-dendrotoxin were determined in a manner similar to that used for characterizing ROMK1. While IRK1 is also an inward rectifier, Kv1.1, Kv1.6, and Shaker are voltage-gated K^+ channels. Clearly δ-dendrotoxin is not specific to a single K^+ channel family and shows variations in affinity even within a given family. These findings suggest that the δ-dendrotoxin binding site has been conserved across K^+ channel families and that binding depends on the specific molecular details of the given channel binding site.

Effects of Pore Mutations on Toxin Binding. To determine whether δ-dendrotoxin inhibits ROMK1 current by binding

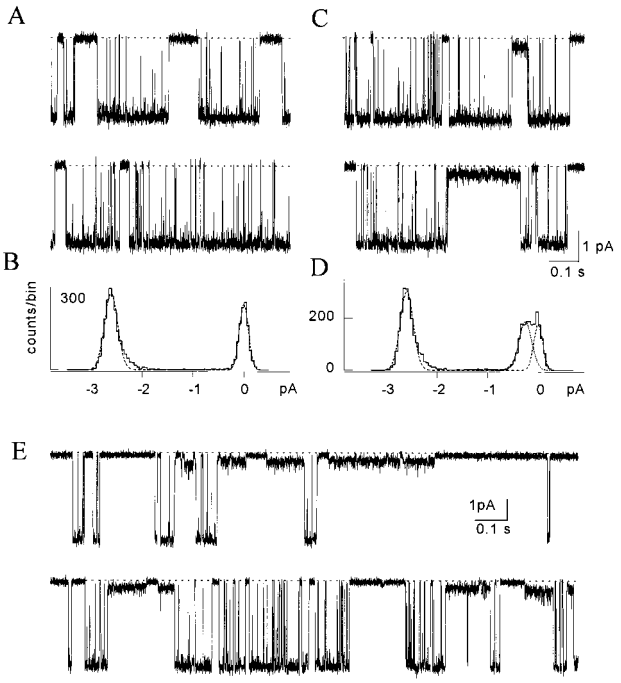

FIGURE 6: Dendrotoxin binding does not inhibit the channel completely. (A) Two sequential 0.82 s current traces of a single ROMK1 channel in the presence of Ba^{2+}. The oocyte-attached patch pipet contained K^+ recording solution and 0.01 mM $BaCl_2$. Holding potential, −80 mV. Dashed line indicates Ba^{2+} blocked current. (B) Amplitude histogram of top trace in (A). Bin width, 0.05 pA. The dashed curve is the fit of the sum of two Gaussian curves centered around mean currents of −2.6 and 0.0 pA with standard deviations of 0.26 and 0.18 pA, respectively. (C) Same as in (A) but from a patch pipet filled with 0.01 mM $BaCl_2$ and δ-dendrotoxin (see Experimental Procedures). Only in the presence of dendrotoxin were closures to a subconductance level observed. These closures were noisier than the Ba^{2+}-induced channel blocks. (D) Amplitude histogram of the second trace in (C) illustrates these differences. The dashed lines show three Gaussian curves whose sum provided the best fit to the histogram. The means of the curves were, from left to right, −2.6, −0.25, and 0 pA, and their respective deviations, 0.25, 0.25, and 0.17 pA. (E) A continuous 3.3 s recording of the same channel shown in (C) at a holding potential of −120 mV. The blocks by dendrotoxin and Ba^{2+} are not mutually exclusive. The Ba^{2+} ion still has access to the pore while dendrotoxin is bound to the channel. Conversely, toxin may bind while Ba^{2+} is blocking the pore. Identical conclusions were reached in four separate patches containing a single ROMK1 channel.

to the pore entryway, the effects of changing amino acids in this region were examined. The first two sequences in Figure 7 compare toxin-insensitive IRK1 and toxin-sensitive ROMK1 in this region. IRK1 and ROMK1 differ by two residues in the signature sequence (Figure 7, shaded boxed region). Comparison of the regions flanking both sides of the signature sequence reveals 24 amino acids that differ between the two channels (lower case letters). Two of these represent a change in the hydrophobic nature of the side chain (residues 110 and 117), seven represent changes in charge (positions 111, 116, 118, 119, 123, 124, and 152), and the remaining differences are chemically more conservative. Selected residues determining differences in either charge or polarity between IRK1 and ROMK1 were altered individually (or as a pair for residues 151 and 152) by site-directed mutagenesis (arrows, Figure 8). The affinity of recombinant δ-dendrotoxin was measured for each mutant channel expressed in oocytes and plotted as the K_d normalized by that of wild-type ROMK1 (Figure 8).

```
ROMK1
Residue#:  110       120       130       140       150        Affinity
Sequence   ..|....'....|..*.'....|....'....|....'....|....'... [δ-dtx],nM
ROMK1:     DLpefyppdnrtpCVeniNgmTsAFLFSlETGVTIGYGFRfVTeqCatAiF  152 ± 10
IRK1:      DLdts---kvsdaCVsevNsfTaAFLFSiETQTTIGYGFRcVTdeCpiAvF   none
Kv1.1:     LFSSAVYFAEAEEAESHFSSIPDAFWWAVVSMTTVGYGDMYPVTIGGKIVG   < 0.1
KV1.6:     LFSSAVYFAEADDVDSLFPSIPDAFWWAVVTMTTVGYGDMYPMTVGGKIVG   23 ± 5
Shaker:    LFSSAVYFAEAGSENSFFKSIPDAFWWAVVTMTTVGYGDMTPVGFWGKIVG   none
```

FIGURE 7: Pore regions of several K^+ channels whose affinities for δ-dendrotoxin differ. Alignment of amino acid sequences of the pore regions linking the outer and inner helices of ROMK1 and IRK1 inward rectifiers and the corresponding S5 and S6 helices in voltage-gated channels Kv1.1, Kv1.6, and Shaker. The boxed shaded region highlights the K^+ channel signature sequences used for the alignment and responsible for K^+ ion selectivity. Lower case letters indicate amino acid differences between toxin-sensitive ROMK1 and toxin-insensitive IRK1. Shaded regions denote amino acids identical in all voltage-gated and at least one of the inward rectifier K^+ channels. Boxed residues in Kv1.1 are those whose substitution has been shown to cause large reductions in the affinity of α-dendrotoxin for this voltage-gated channel (*29*). The asterisk denotes the position of the glutamate residue in ROMK1 necessary for binding of δ-dendrotoxin. Affinity is reported as K_d ($n = 3-18$ measurements).

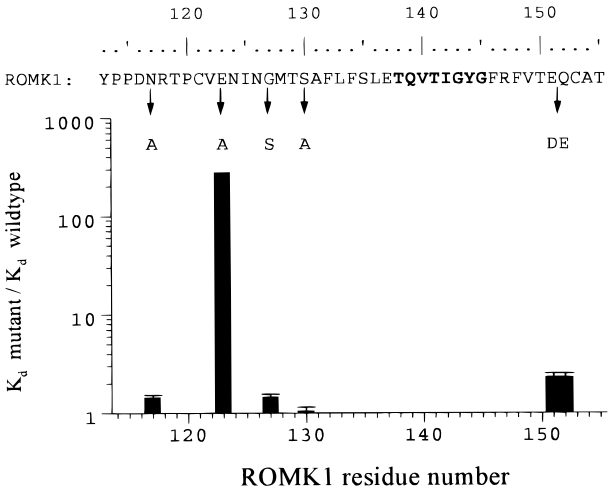

FIGURE 8: Mutations in the ROMK1 channel pore affect δ-dendrotoxin affinity. (Top) Numbered amino acid sequence of the pore region of ROMK1. Boldface residues identify the K^+ channel signature sequence. Arrows indicate the amino acid substitutions made. (Bottom) Plotted are the half-maximal block concentrations of δ-dendrotoxin for ROMK1 mutants relative to wild-type channels. No significant block (more than 5% of control current) was seen in E123A with 100 nM ($n = 3$) or 500 nM ($n = 2$) δ-dendrotoxin. The K_d value for this toxin was determined with a single measurement at 10 μM toxin. Other K_d values were as follows: N117A, 220 ± 10, $n = 5$; G127S, 221 ± 15, $n = 5$; S130A, 160 ± 14, $n = 5$; E151D/Q152E, 350 ± 30, $n = 5$. Relative affinities were calculated using a wild-type ROMK1 K_d of 150 nM.

The results from the point-mutation studies indicate that all but one of the mutated residues altered the binding affinity of δ-dendrotoxin to ROMK1. The largest effect was seen with the substitution of glutamate 123 by alanine, which lowered the affinity to $K_d \cong 40$ μM. Concentrations in the range of 100−200 nM did not perceptibly block this mutant channel.

DISCUSSION

We have purified and identified a snake venom inhibitor of the inward rectifier K^+ channel ROMK1. The identity of this inhibitor is δ-dendrotoxin. Recombinant synthesis of this toxin in *E. coli* allowed the electrophysiological characterization of δ-dendrotoxin affinity to wild-type ROMK1 and identification of a ROMK1 region which is involved in binding of the toxin. A single-residue change in ROMK1, E123A, altered the toxin affinity by more than 2 orders of magnitude. Figure 7 illustrates the relative position of E123A of ROMK1 to those residues in Kv1.1 whose mutation changes the affinity of α-dendrotoxin (*29*). Changes in the toxin binding energy as a result of several point mutations within the extracellular entryway of ROMK1 indicate that δ-dendrotoxin binds to the pore region of this channel and that a key interaction between toxin and channel is electrostatic. The electrostatic component of the interaction of δ-dendrotoxin with the inward rectifier parallels well-characterized interactions of pore-blocking scorpion toxins with K^+ channels.

δ-Dendrotoxin's failure to block ROMK1 completely was unexpected. Two pieces of evidence support the conclusion that the toxin only partially blocks the ROMK1 channel when bound. First, some of the additional current blocked by near-saturating concentrations of LQ2 (from 25% to 10% of control current, Figure 4, c,d) can be recovered by concurrent application of high concentrations of δ-dendrotoxin. Since LQ2 has been shown to interact with the pore region of ROMK1 (*25*) and the δ-dendrotoxin receptor site involves residues in the same region, they must compete for apparently overlapping sites. Second, when Ba^{2+} and toxin are present in the patch pipet, the toxin-bound channel displays a conductance level that is distinct from that of Ba^{2+} alone (Figure 6). That is, δ-dendrotoxin induces a substate.

While δ-dendrotoxin binds to the external vestibule of the channel, it does not block the pore in the same way that other "pore blocking" toxins are thought to achieve block of the channel. There are several possible ways that binding without complete occlusion of the pore may occur. One is that the toxin, when bound to the channel, may only partially shield the pore entryway either electrostatically or sterically, leading to a decrease in the rate of diffusion of the permeant K^+ ion into the selectivity filter. Another is that the bound toxin induces slight changes in the selectivity filter conformation resulting in changes in ion−ion interaction within the pore and therefore a reduced flux. The fact that Ba^{2+} still binds to the toxin-bound channel rules out large conformational changes in the selectivity filter. Finally, the toxin may bind to the channel and change the dynamic equilibrium gating of the channel to favor the closed state of the channel. If during binding of the toxin the transitions between the native closed state and the native open state of the channel are sufficiently rapid, the strong filtering of our current signal would make such gating look like a subconductance state. Curiously, a recent study of the affinity of dendrotoxin homologues to K^+ channel Kv1.1 expressed in

Chinese hamster ovary (CHO) cells has reported that both β- and γ-dendrotoxins are not able to block the Kv1.1 current completely at high concentrations even though their affinities are in the nanomolar range (*41*). Clearly, this characteristic of the dendrotoxins merits further study and clarification.

The finding that δ-dendrotoxin interacts with both inward rectifiers and voltage-dependent K^+ channels reveals that the structure of the outer face of the channel may have been conserved across K^+ channel classes despite strong divergence of the amino acid sequences flanking the signature sequence (Figure 7). Recently, the X-ray structure of a K^+ channel from *Streptomyces lividans* (*11*) has revealed the distinct topographical features of the outer face. Among these are four prominent loops or turrets on each of the four corners of the face formed by the channel tetramer. These turrets are shown to cradle agitoxin, centered between them, when the toxin binds to the channel (*44*). It is quite likely that dendrotoxin, which is larger and more elongate (*45*, *46*) in shape than agitoxin, will interact more extensively with amino acids in the turret. The study of the interaction of dendrotoxin with its channel receptor promises to reveal new information regarding K^+ channel structure and function.

ACKNOWLEDGMENT

We thank Z. Lu (University of Pennsylvania) for the gift of recombinant LQ2 scorpion toxin and ROMK1 cDNA mutants, and J. Rush (Harvard HHMI Biopolymer Facility) for the amino acid analysis, mass spectrometry, and peptide sequencing. R.M. is an Investigator in the Howard Hughes Medical Institute.

REFERENCES

1. Kubo, Y. (1994) *Neurosci. Res. 21*, 109−117.
2. Doupnik, C. A., Davidson, N., and Lester, H. A. (1995) *Curr. Opin. Neurobiol. 5*, 268−277.
3. Ho, K., Nichols, C. G., Lederer, W. J., Lytton, J., Vassilev, P. M., Kanazirska, M. V., and Hebert, S. C. (1993) *Nature 362*, 31−38.
4. Kubo, Y., Baldwin, T. J., Jan, Y. N., and Jan, L. Y. (1993) *Nature 362*, 127−133.
5. Kubo, Y., Reuveny, E., Slesinger, P. A., Jan, Y. N., and Jan, L. Y. (1993) *Nature 364*, 802−806.
6. Wible, B. A., De Biasi, M., Majumder, K., Taglialatela, M., and Brown, A. M. (1995) *Circ. Res. 76*, 343−350.
7. Krapivinsky, G., Gordon, E. A., Wickman, K., Velimirovic, B., Krapivinsky, L., and Clapham, D. E. (1995) *Nature 374*, 135−141.
8. Makhina, E. N., Kelly, A. J., Lopatin, A. N., Mercer, R. W., and Nichols, C. G. (1994) *J. Biol. Chem. 269*, 20468−20474.
9. Takahashi, N., Morishige, K., Jahangir, A., Yamada, M., Findlay, I., Koyama, H., and Kurachi, Y. (1994) *J. Biol. Chem. 269*, 23274−23279.
10. Jan, L. Y., and Jan, Y. N. (1997) *Annu. Rev. Neurosci. 20*, 91−123.
11. Doyle, A. D., Morais Cabral, J., Pfuetzner, R. A., Kuo, A., Gulbis, J. M., Cohen, S. L., Chait, B. T., and MacKinnon, R. (1998) *Science 280*, 69−77.
12. Lu, Z., and MacKinnon, R. (1994) *Nature 371*, 243−246.
13. Vandenberg, C. A. (1987) *Proc. Natl. Acad. Sci. U.S.A. 84*, 2560−2564.
14. MacKinnon, R., and Miller, C. (1989) *Science 245*, 1382−1385.
15. MacKinnon, R., Heginbotham, L., and Abramson, T. (1990) *Neuron 5*, 767−771.
16. MacKinnon, R. (1991) *Nature 350*, 232−235.
17. Goldstein, S. A. N., Pheasant, D. J., and Miller, C. (1994) *Neuron 12*, 1377−1388.
18. Stampe, P., Kolmakova-Partensky, L., and Miller, C. (1994) *Biochemistry 33*, 443−450.
19. Stocker, M., and Miller, C. (1994) *Proc. Natl. Acad. Sci. U.S.A. 91*, 9509−9513.
20. Hidalgo, P., and MacKinnon, R. (1995) *Science 268*, 307−310.
21. Naranjo, D., and Miller, C. (1996) *Neuron 16*, 123−130.
22. Aiyar, J., Rizzi, J. P., Gutman, G. A., and Chandy, K. G. (1996) *J. Biol. Chem. 271*, 31013−31016.
23. Ranganathan, R., Lewis, J. H., and MacKinnon, R. (1996) *Neuron 16*, 131−139.
24. Gross, A., and MacKinnon, R. (1996) *Neuron* 16, 399−406.
25. Lu, Z., and MacKinnon, R. (1997) *Biochemistry 36*, 6936−6940.
26. Awan, K. A., and Dolly, J. O. (1991) *Neuroscience 40*, 29−39.
27. Rehm, H., and Lazdunski, M. (1988) *Proc. Natl. Acad. Sci. U.S.A. 85*, 4919−4923.
28. Parcej, D. N., and Dolly, J. O. (1989) *Biochem. J. 257*, 899−903.
29. Hurst, R. S., Busch, A. E., Kavanaugh, M. P., Osborne, P. B., North, R. A., and Adelman, J. P. (1991) *Mol. Pharmacol. 40*, 572−576.
30. Stocker, M., Pongs, O., Hoth, M., Heinemann, S. H., Stuhmer, W., Schroter, K. H., and Ruppersberg, J. P. (1991) *Proc. R. Soc. London B, Biol. Sci. 245*, 101−107.
31. Tytgat, J., Debont, T., Carmeliet, E., and Daenens, P. (1995) *J. Biol. Chem. 270*, 24776−24781.
32. Harvey, A. L. (1997) *Gen. Pharmacol. 28*, 7−12.
33. Park, C. S., Hausdorff, S. F., and Miller, C. (1991) *Proc. Natl. Acad. Sci. U.S.A. 88*, 2046−2050.
34. Sanger, F., Nicklen, S., and Coulson, A. R. (1977) *Proc. Natl. Acad. Sci. U.S.A. 74*, 5463−5467.
35. Dunn, J. J., and Studier, F. W. (1983) *J. Mol. Biol. 166*, 477−535.
36. Kamb, A., Iverson, L. E., and Tanouye, M. A. (1987) *Cell 50*, 405−413.
37. Stühmer, W., Stocker, M., Sakmann, B., Seeburg, P., Baumann, A., Grupe, A., and Pongs, O. (1988) *FEBS Lett. 242*, 199−206.
38. Swanson, R., Marshall, J., Smith, J. S., Williams, J. B., Boyle, M. B., Folander, K., Luneau, C. J., Antanavage, J., Oliva, C., Buhrow, S. A., et al. (1990) *Neuron 4*, 929−939.
39. Joubert, F. J., and Taljaard, N. (1980) *Hoppe-Seylers' Z. Physiol. Chem. 361*, 661−674.
40. Benishin, C. G., Sorensen, R. G., Brown, W. E., Krueger, B. K., and Blaustein, M. P. (1988) *Mol. Pharmacol. 34*, 152−159.
41. Hall, A., Stow, J., Sorensen, R., Dolly, J. O., and Owen, D. (1994) *Br. J. Pharmacol. 113*, 959−967.
42. Owen, D. G., Hall, A., Stephens, G., Stow, J., and Robertson, B. (1997) *Br. J. Pharmacol. 120*, 1029−1034.
43. Hedin, K. E., Lim, N. F., and Clapham, D. E. (1996) *Neuron 16*, 423−429.
44. MacKinnon, R., Cohen, S. L., Kuo, A., Lee, A., and Chait, B. T. (1998) *Science 280*, 106−109.
45. Skarzynski, T. (1992) *J. Mol. Biol. 224*, 671−683.
46. Berndt, K. D., Guntert, P., and Wuthrich, K. (1993) *J. Mol. Biol. 234*, 735−750.

BI980929K